Clinical, Cosmetic and Investigational Dermatology

Dovepress
Taylor & Francis Group

Open Access Full Text Article

ORIGINAL RESEARCH

Diagnostic Performance of High-Frequency Ultrasound and Ultra-High-Frequency Ultrasound in Distinguishing Dermatofibrosarcoma Protuberans from Dermatofibroma: A 15-year Period Retrospective Analysis

Guiwu Chen[1,*], Haibo Luo[1,*], Wenqin Liu[1], Xiaomin Liao[2], Jiaxin Meng[1], Zhongxian Qiu[1], Xiaoling Leng[1]

[1]Department of Ultrasound, The Tenth Affiliated Hospital, Southern Medical University, Dongguan People's Hospital, Dongguan, People's Republic of China; [2]Department of Pathology, The Tenth Affiliated Hospital, Southern Medical University, Dongguan People's Hospital, Dongguan, People's Republic of China

*These authors contributed equally to this work

Correspondence: Xiaoling Leng, Department of Ultrasound, The Tenth Affiliated Hospital, Southern Medical University, Dongguan People's Hospital, 3 South Wandao Road, Wanjiang District, Dongguan, Guangdong, 523059, People's Republic of China, Tel +86 13899950268, Fax +86 076928636378, Email lengxiaoling60017@163.com

Purpose: Dermatofibrosarcoma protuberans (DFSP) and dermatofibroma (DF) are cutaneous lesions with overlapping clinical features, often requiring histopathological confirmation. This study aims to evaluate and compare the diagnostic utility of high-frequency ultrasound (HFUS) and ultra-high-frequency ultrasound (UHFUS) in distinguishing these two entities over 15-year period.

Methods: A retrospective analysis was conducted on 334 patients (127 DFSP, 207 DF) with pathologically confirmed diagnoses. HFUS or UHFUS was used to assess lesion characteristics, including demographics, location, size, morphology, echogenicity, homogeneity, posterior acoustic features, and vascularity. Univariate and multivariate logistic regression analyses were performed to identify significant predictors.

Results: DFSP patients were significantly older than DF patients (40.99 years vs 34.00 years; $P < 0.001$). DFSP lesions were predominantly on the trunk, while DF was more common on the extremities ($P < 0.001$). DFSP lesions were significantly larger (mean 43.02 mm vs 10.34 mm; $P < 0.001$), and exhibited more aggressive sonographic features, including tentacle-like borders, internal hyperechoic areas, peripheral hyperechoic rims, mixed echogenicity, irregular shape, ill-defined margins, internal heterogeneity, and frequent posterior enhancement (all $P < 0.005$). DFSP also showed higher vascularity with random, peripheral, or arborizing patterns and higher Adler grades (all $P < 0.001$). Multivariate analysis identified tumor location (extremities favoring DF), size, ultrasound pattern (tentacle-like border pattern, internal hyperechoic area, peripheral hyperechoic rim, and mixed echogenicity pattern favoring DFSP) as independent predictors.

Conclusion: HFUS and UHFUS demonstrates strong diagnostic utility in differentiating DFSP from DF based on key clinical and sonographic features. These findings support the use of HFUS and UHFUS as a valuable non-invasive tool for preoperative diagnosis. Future studies should validate these criteria in multi-center settings and exploring artificial intelligence integration to further enhance diagnostic accuracy and standardization.

Keywords: dermatofibroma, dermatofibrosarcoma protuberans, high-frequency ultrasound, ultra-high-frequency ultrasound, pathological examination

Received: 19 October 2025
Accepted: 24 December 2025
Published: 28 December 2025

Introduction

Dermatofibroma (DF) and dermatofibrosarcoma protuberans (DFSP) are two distinct cutaneous lesions that often present diagnostic challenges due to their overlapping clinical and imaging features.[1] DF, a benign fibrous histiocytoma, is one of the most common superficial skin lesions, typically presenting as a small, firm nodule.[2] In contrast, DFSP is a rare, low- to intermediate-grade sarcoma characterized by its locally aggressive behavior and high recurrence rate if not adequately excised.[3] Accurate differentiation between these two entities is crucial for appropriate clinical management, as DFSP requires wide surgical excision to prevent recurrence, while DF can often be managed conservatively.[4,5]

Ultrasound imaging, particularly high-frequency ultrasound (HFUS) and ultra-high-frequency ultrasound (UHFUS), has emerged as a valuable tool in the evaluation of superficial soft tissue lesions.[6] HFUS provides excellent visualization of the dermis and subcutaneous tissue, while UHFUS, operating at even higher frequencies (typically 20–100 MHz), further improves spatial resolution, enabling more detailed characterization of cutaneous structures.[7] This high-resolution imaging capability allows for the precise assessment of lesion depth, margins, and internal echogenicity, which are critical in distinguishing between benign and malignant cutaneous tumors.[8]

Previous studies have highlighted the utility of ultrasound in characterizing DF and DFSP. DF typically appears on ultrasound as an ill-defined, hypoechoic lesion in the dermis or upper hypodermis, often with spiculated margins and changes in adjacent soft tissue echogenicity.[9,10] In contrast, DFSP often presents as a hypoechoic mass with irregular borders, tentacle-like projections, and hypervascularity, reflecting its infiltrative growth pattern.[11,12] However, the diagnostic accuracy of ultrasound in differentiating these two entities, particularly using HFUS and UHFUS, has not been extensively studied over extended periods.[13,14] Large-scale, long-term retrospective studies specifically evaluating the diagnostic performance of HFUS and UHFUS in differentiating DF from DFSP are scarce.

This retrospective analysis aims to evaluate the utility of HFUS and UHFUS in distinguishing between DF and DFSP over 15 years. By examining a large cohort of patients, we seek to identify specific sonographic features that can aid in the accurate diagnosis and management of these lesions, thereby facilitating appropriate surgical planning and potentially reducing recurrence rates.

Materials and Methods

Study Design and Population

This retrospective study was conducted using data from the Pathology Report System of Dongguan People's Hospital from November 2009 to July 2025. The initial cohort comprised 899 surgically treated and pathologically confirmed patients, including 691 diagnosed with DF and 208 with DFSP. The final analytical cohort was derived from this group and consisted of 334 patients, specifically 207 DF cases and 127 DFSP cases, for whom HFUS or UHFUS images were available in the Picture Archiving and Communication System (Figure 1).

The inclusion criteria comprised: (1) pathologically confirmed diagnosis of DF or DFSP; (2) availability of complete preoperative HFUS or UHFUS imaging data; (3) no previous treatment or intervention before ultrasound examination. Exclusion criteria were: (1) incomplete clinical or imaging records; (2) history of surgical excision or other treatments prior to ultrasound evaluation.

Acquisition of Ultrasound Images

Before each examination, patients were instructed to expose the skin lesions in the appropriate position. To enhance image quality, a generous amount of ultrasound gel was applied between the transducer and the lesion surface. All lesions were first scanned using HFUS for initial lesion localization and comprehensive assessment, providing greater penetration depth for evaluating deeper tissue involvement. Subsequently, UHFUS was primarily employed to depict superficial anatomical structures and lesion details with high resolution. Grayscale ultrasound images were acquired by scanning all lesions, followed by a color Doppler flow imaging to visualize the internal blood flow. The HFUS and UHFUS settings, including depth, gain, focus, and frequency, were carefully adjusted to ensure a clear depiction of the lesions. The soft tissues were meticulously scanned for any lesions, and their locations were precisely marked on the ultrasound image.

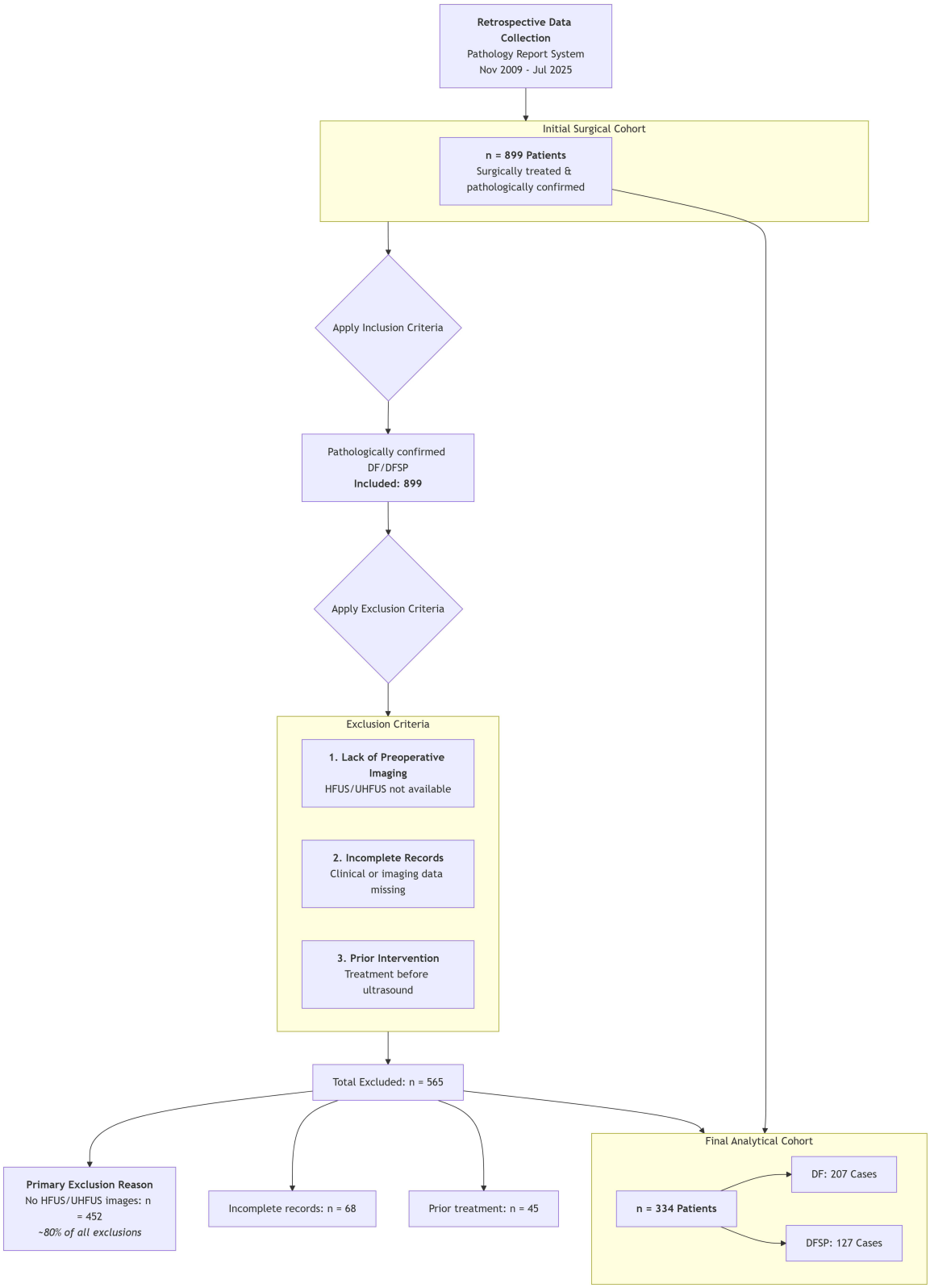

Figure 1 Patient selection flowchart for the retrospective study.

https://doi.org/10.2147/CCID.S575360

Representative images were securely saved in the informatics database of the Picture Archiving and Communications System for further analysis and documentation.

Interpretation of Ultrasound Images

On grayscale ultrasound imaging, various characteristics of the lesions were evaluated, including size, shape (regular, irregular), margin (well-defined, ill-defined), internal echogenicity (hypoechoic, isoechoic, hyperechoic), homogeneity (homogeneous, heterogeneous), and posterior acoustic features (no change, attenuation, enhancement). Based on the aforementioned sonographic features, the lesions were further categorized into specific ultrasound patterns: compressive pattern, serrated pattern, tentacle-like border pattern, internal hyperechoic area, peripheral hyperechoic rim, mixed echogenicity pattern, all of which were illustrated in Figure 2.

Color Doppler flow imaging was performed by superimposing color pixels onto grayscale ultrasound images to evaluate the presence and characteristics of blood flow in real-time. The diagnostic criteria for color doppler flow imaging were established as follows: Adler grade 0, indicating absence of blood flow and no vascularization; Adler grade 1, representing minimal vascularization with one or two pixels containing flow; Adler grade 2, demonstrating moderate vascularization with one main or several small blood vessels; and Adler grade 3, indicating rich vascularization with more than two main or four small blood vessels. The spatial distribution of the largest diameter blood flow was categorized into specific patterns (absent, arborizing, peripheral, random).

Statistical Analysis

Statistical analyses were performed using SPSS software (version 26.0, IBM Corp, Armonk, NY, USA). Continuous variables, such as age and lesion size, were presented as mean ± standard deviation and compared using independent samples *t*-tests. Categorical variables, including gender, lesion location, shape, margin, internal echogenicity, homogeneity, posterior acoustic features, ultrasound patterns, blood flow patterns, and blood flow grading, were expressed as frequencies and percentages. Inter-rater reliability for the Ultrasound pattern was evaluated using Cohen's kappa. Group differences for categorical variables were assessed using the chi-square (χ^2) test or Fisher's exact test, as appropriate.

Univariate logistic regression analysis was conducted to identify potential predictors of DFSP and DF. We tested for collinearity using the variance inflation factor (VIF) and defined problematic collinearity as a VIF > 5. Variables with *P*-values < 0.05 in the univariate analysis were included in the multivariate logistic regression model to determine independent predictors of DFSP. Odds ratios (*ORs*) and 95% confidence intervals (*CIs*) were calculated to quantify the strength of associations. A two-tailed *P*-value < 0.05 was considered statistically significant.

Results

Patient Demographics and Clinical Characteristics

A total of 334 patients were included in the study, comprising 207 cases of DF and 127 cases of DFSP. The mean age of DF patients was significantly younger than DFSP patients (34.00 ± 12.270 years vs 40.99 ± 13.95 years; $t = 4.794$, $P < 0.001$). Gender distribution showed no significant difference between the two groups ($\chi^2 = 3.351$, $P = 0.067$), with 96 males and 111 females in the DF group, and 72 males and 55 females in the DFSP group.

The anatomical distribution of lesions differed significantly between DF and DFSP ($\chi^2 = 43.309$, $P < 0.001$). DF lesions were more commonly located on the limbs (head: 12 cases; girdle: 34 cases; limb: 101 cases), whereas DFSP lesions predominated in the trunk (77 cases) (Table 1).

Ultra-High-Frequency and High-Frequency Sonographic Features

The mean lesion size was significantly larger in DFSP compared to DF (43.02 ± 39.47 mm vs 10.34 ± 7.07 mm; $t = 9.240$, $P < 0.001$). Morphologically, DF lesions were more often regular and well-defined, whereas DFSP lesions tended to be irregular (78 cases vs 58 cases; $\chi^2 = 36.371$, $P < 0.001$) and ill-defined (63 cases vs 77cases; $\chi^2 = 4.977$, $P = 0.026$). Internal echogenicity was predominantly hypoechoic in both groups, but DFSP showed higher heterogeneity (117 cases vs 79 cases; $\chi^2 = 94.527$, $P < 0.001$). Posterior acoustic features also differed, with DFSP more frequently exhibiting

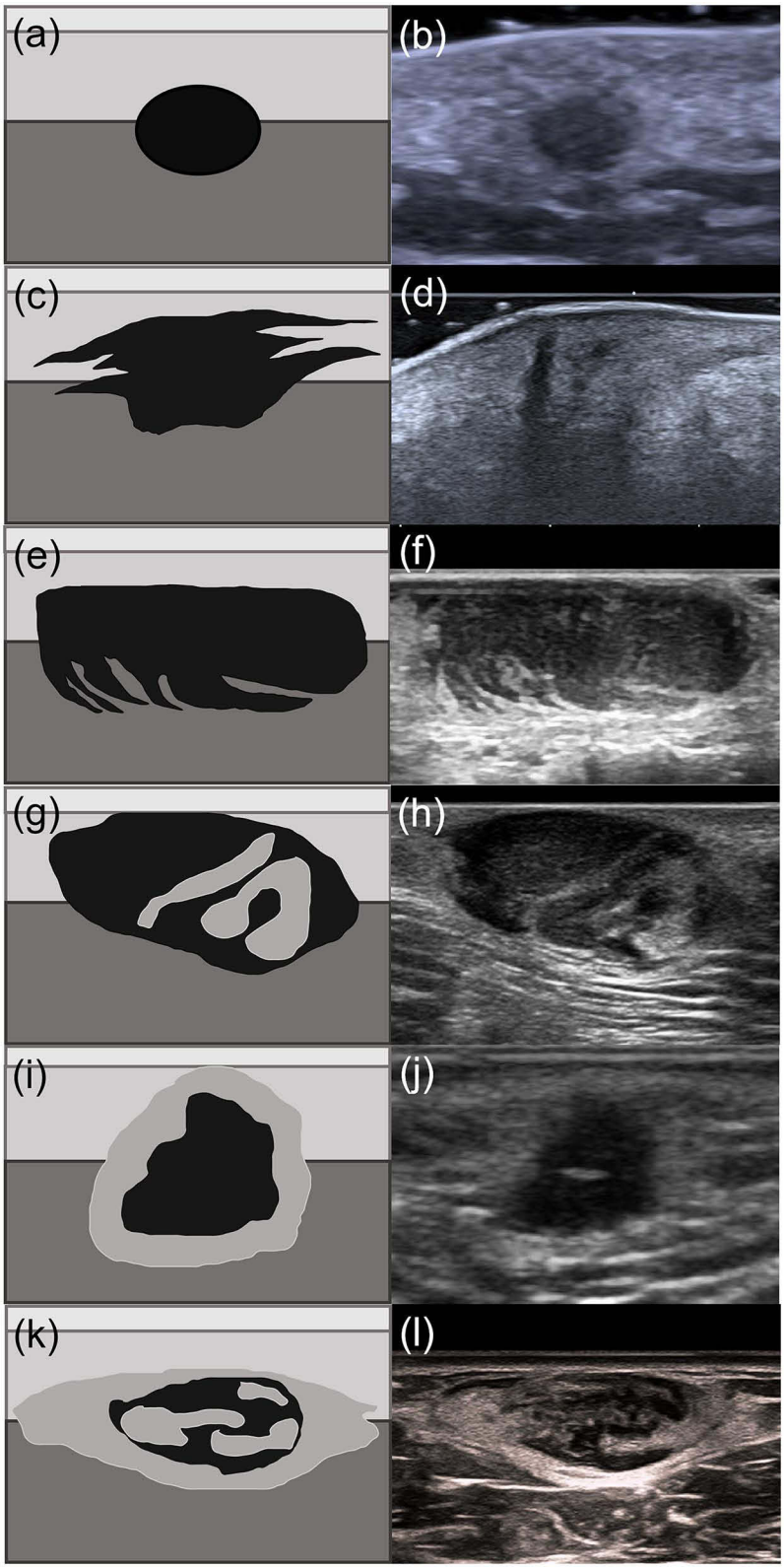

Figure 2 Ultrasound patterns of dermatofibrosarcoma protuberans and dermatofibroma. Schematic illustrations (left) and corresponding grayscale ultrasound images (right) are provided for each pattern. (**a** and **b**) Compressive pattern: A well-defined, regularly shaped lesion exhibiting homogeneous echotexture. (**c** and **d**) Serrated pattern: An ill-defined lesion with serrated margins, showing homogeneous echotexture. (**e** and **f**) Tentacle-like border pattern: A lesion with tentacle-like extensions invading the subcutaneous tissue, displaying either homogeneous or heterogeneous echotexture. (**g** and **h**) Internal hyperechoic area: A lesion containing internal hyperechoic areas, which may appear regular or irregular in shape. (**i** and **j**) Peripheral hyperechoic rim: An irregular lesion surrounded by a hyperechoic rim. (**k** and **l**) Mixed echogenicity pattern: A lesion demonstrating multiple characteristic features, including tentacle-like extensions, internal hyperechoic areas, and a peripheral hyperechoic rim.

Table 1 Patient Demographics and Clinical Characteristics

	Total	Dermatofibrosarcoma Protuberans	Dermatofibroma	t/χ^2	*P*
Age (year)	36.66±13.35	40.99±13.95	34.00±12.27	4.794	<0.001
Gender				3.351	0.067
Male	168	72	96		
Female	166	55	111		
Tumor location				43.309	<0.001
Head	17	5	12		
Neck	12	6	6		
Girdle	45	11	34		
Trunk	131	77	54		
Limb	129	28	101		

enhancement (67 cases vs 61 cases; $\chi^2 = 20.038$, $P < 0.001$). Distinct ultrasound patterns differentiated DF and DFSP lesions ($\chi^2 = 114.318$, $P < 0.001$). DF lesions were predominantly either compressive (n=136) or serrated (n=38), whereas DFSP lesions most commonly exhibited tentacle-like borders (n=22), internal hyperechoic areas (n=30), a peripheral hyperechoic rim (n=15), or mixed echogenicity (n=24). Interobserver agreement for the ultrasound pattern classification was substantial interobserver agreement, with a Kappa value of 0.893 ($P < 0.001$).

Blood flow analysis demonstrated significant differences in vascular patterns. DF lesions were often avascular (162 cases), while DFSP lesions displayed random (67 cases), peripheral (21 cases), and arborizing (13 cases) distributions ($\chi^2 = 109.577$, $P < 0.001$). Blood flow grading further distinguished DFSP, with higher Adler grades compared to DF (101 cases vs 45 cases; $\chi^2 = 107.999$, $P < 0.001$) (Table 2).

Table 2 Ultra-High-Frequency and High-Frequency Sonographic Features

	Total	Dermatofibrosarcoma Protuberans	Dermatofibroma	t/χ^2	*P*
Size (mm)	22.76±29.54	43.02±39.47	10.34±7.07	9.240	<0.001
Shape				36.371	<0.001
Regular	198	49	149		
Irregular	136	78	58		
Margin				4.977	0.026
Well-defined	194	64	130		
Ill-defined	140	63	77		
Internal echogenicity				8.536	0.014
Hypoechoic	321	118	203		
Isoechoic	5	2	3		
Hyperechoic	8	7	1		

(*Continued*)

Table 2 (Continued).

	Total	Dermatofibrosarcoma Protuberans	Dermatofibroma	t/χ^2	*P*
Homogeneity				94.527	<0.001
Homogeneous	138	10	128		
Heterogeneous	196	117	79		
Posterior acoustic features				20.038	<0.001
No change	195	59	136		
Attenuation	11	1	10		
Enhancement	128	67	61		
Ultrasound patterns				114.318	<0.001
Compressive pattern	168	32	136		
Serrated pattern	42	4	38		
Tentacle-like border pattern	30	22	8		
Internal hyperechoic area	36	30	6		
Peripheral hyperechoic rim	29	15	14		
Mixed echogenicity pattern	29	24	5		
Blood flow pattern				109.577	<0.001
Absent	188	26	162		
Arborizing	24	13	11		
Peripheral	29	21	8		
Random	93	67	26		
Blood flow grading				107.999	<0.001
Grade 0	188	26	162		
Grade 1	37	23	14		
Grade 2	53	37	16		
Grade 3	56	41	15		

Multivariate Analysis of Patient Demographics, Clinical Characteristics, and Sonographic Features

The multicollinearity assessment showed that the variance inflation factor (VIF) values for all included variables were below 5. This confirms the absence of substantial multicollinearity among the predictors and supports their appropriateness for inclusion in the multivariate logistic regression model (Table 3). Multivariate logistic regression analysis revealed that tumor location, size, and ultrasound pattern were significant predictors of DF and DFSP. Specifically, girdle and limb (*OR* = 0.078, 0.079; *P* = 0.003, < 0.001) showed strong associations with DF, while size, tentacle-like border pattern, internal hyperechoic area, peripheral hyperechoic rim, and mixed echogenicity pattern (*OR* = 1.174, 4.391, 9.155, 9.328, 50.644; *P* < 0.001, 0.046,

Table 3 Multicollinearity Check of Patient Demographics, Clinical Characteristics, and Ultrasound Image Features

Parameters	Unstandardized Coefficients		Standardized Coefficients	t	P	Collinearity Statistics	
	B	*Std. Error*	*B*			*Tolerance*	*VIF*
Age	0.001	0.001	0.017	0.425	0.671	0.807	1.240
Size	0.004	0.001	0.234	5.266	<0.001	0.687	1.455
Location	−0.141	0.086	−0.064	−1.637	0.103	0.893	1.120
Head	−0.033	0.100	−0.013	−0.329	0.743	0.921	1.085
Neck	−0.184	0.059	−0.130	−3.149	0.002	0.797	1.255
Girdle	−0.224	0.042	−0.224	−5.344	<0.001	0.766	1.306
Limb	−0.057	0.057	−0.039	−1.002	0.317	0.894	1.119
Ultrasound pattern	0.278	0.071	0.163	3.904	<0.001	0.771	1.297
Serrated pattern	0.374	0.064	0.239	5.818	<0.001	0.801	1.248
Tentacle-like border pattern	0.204	0.067	0.119	3.056	0.002	0.898	1.113
Internal hyperechoic area	0.363	0.070	0.210	5.185	<0.001	0.821	1.219
Peripheral hyperechoic rim	0.264	0.078	0.141	3.403	0.001	0.792	1.262
Mixed echogenicity pattern	0.301	0.070	0.175	4.290	<0.001	0.816	1.226
Blood flow pattern	0.293	0.048	0.271	6.062	<0.001	0.679	1.474
Arborizing	0.001	0.001	0.017	0.425	0.671	0.807	1.240
Peripheral	0.004	0.001	0.234	5.266	<0.001	0.687	1.455
Random	−0.141	0.086	−0.064	−1.637	0.103	0.893	1.120
Constant	0.155	0.063		2.471	0.014		

0.002, 0.003, < 0.001) showed strong associations with DFSP. However, blood flow pattern did not demonstrate independent significance in the multivariate model (Table 4). The sensitivity, specificity, Youden's index, and area under the curve of the multivariate model were 0.858, 0.971, 0.829, and 0.970, respectively (Figure 3).

Table 4 Univariate and Multivariate Analysis of Patient Demographics, Clinical Characteristics, and Ultrasound Image Features

Parameters	*B*	*SE*	*Wals*	*df*	*P*	*OR*	95% CI	
							Lower Limit	Upper Limit
Age	0.024	0.019	1.506	1	0.220	1.024	0.986	1.064
Size	0.161	0.028	33.156	1	<0.001	1.174	1.112	1.240
Location			21.071	4	<0.001			
Head	−1.059	0.967	1.199	1	0.274	0.347	0.052	2.308
Neck	−1.718	1.482	1.344	1	0.246	0.179	0.010	3.276
Girdle	−2.556	0.867	8.680	1	0.003	0.078	0.014	0.425
Limb	−2.544	0.581	19.171	1	<0.001	0.079	0.025	0.245

(*Continued*)

Table 4 (Continued).

Parameters	*B*	*SE*	*Wals*	*df*	*P*	*OR*	95% CI	
							Lower Limit	Upper Limit
Ultrasound pattern			16.112	5	0.007			
Serrated pattern	0.352	0.843	0.175	1	0.676	1.422	0.273	7.418
Tentacle-like border pattern	1.480	0.742	3.974	1	0.046	4.391	1.025	18.808
Internal hyperechoic area	2.214	0.717	9.544	1	0.002	9.155	2.247	37.307
Peripheral hyperechoic rim	2.233	0.752	8.819	1	0.003	9.328	2.137	40.725
Mixed echogenicity pattern	3.925	0.869	20.411	1	<0.001	50.644	9.227	277.971
Blood flow pattern			7.269	3	0.064			
Arborizing	1.549	0.842	3.383	1	0.066	4.706	0.903	24.520
Peripheral	0.482	0.776	0.386	1	0.534	1.620	0.354	7.420
Random	1.404	0.582	5.824	1	0.016	4.071	1.302	12.729
Constant	−4.656	0.873	28.417	1	<0.001	0.010		

Discussion

Demographic and Clinical Distinctions

This study provides a comprehensive evaluation of HFUS and UHFUS in DF from DFSP, two cutaneous lesions that frequently present diagnostic challenges. Clinically, DF typically appears as small, firm, slow-growing nodules predominantly found on the extremities of young to middle-aged women.[15,16] In contrast, DFSP manifests as larger, progressively enlarging plaques or nodules primarily occurring in adults aged 30–50 years, with no gender predilection.[17,18] Anatomically, DF predominantly affects the head, girdle, limb, while DFSP favors the trunk. These patterns provide valuable diagnostic clues: extremity lesions with typical features likely represent DF, whereas truncal lesions should raise suspicion for DFSP.[19,20] These findings may reflect DF's association with minor trauma (common on extremities) versus DFSP's potential embryological origin (explaining truncal predominance). These clinical differences, while helpful, often require imaging confirmation for accurate diagnosis.

Sonographic Differentiation Features

Our imaging findings underscore sonographic features of DFSP and DF as visualized by HFUS and UHFUS. DF typically manifests as hypoechoic nodules with poorly defined margins, regular contours, and spiculated borders, often accompanied by altered adjacent tissue echogenicity, reflecting its benign fibrous proliferation and chronic inflammatory nature. These features correlate with its indolent clinical course, rarely requiring extensive intervention.[21] In contrast, DFSP exhibits more aggressive features, including an irregular tentacle-like border and marked hypervascularity, reflecting its infiltrative growth pattern.[22] The tumor frequently exhibits heterogeneous echotexture, posterior acoustic changes, and prominent vascularity with higher blood flow grades, all of which align with its malignant potential and propensity for local recurrence if not adequately resected. Notably, certain sonographic patterns, such as internal hyperechoic foci and mixed echogenicity, are more frequently associated with DFSP, while compressive patterns and homogeneous echotexture are more typical of DF.[23–25] The findings emphasize the utility of HFUS and UHFUS in characterizing these tumors, particularly in assessing morphological details, vascular patterns, and depth of invasion, which are critical for clinical management. Compared to HFUS, UHFUS allowed visualization of subtle architectural details that HFUS or earlier studies could not reliably depict. Specifically, UHFUS enhanced the delineation of fine internal reflectivity within lesions, improved border definition—particularly in small (<10 mm) or superficially located

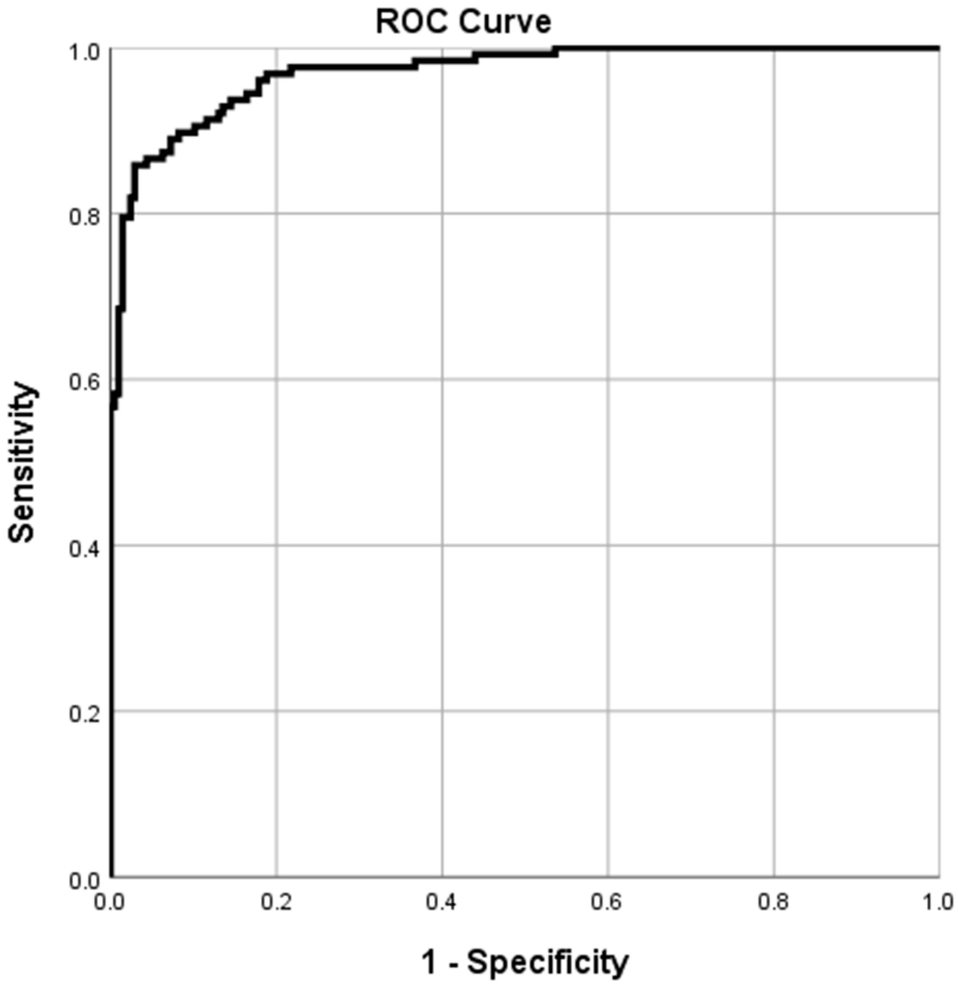

Figure 3 ROC curve of the multivariate model.

tumors—and more clearly revealed subtle tentacle-like projections infiltrating the subcutaneous septum. These capabilities are crucial for distinguishing early or small DFSP from benign mimics like DF, where margin assessment is critical.

Multivariate Predictive Modeling

Our multivariate analysis identified key predictors of DF and DFSP: location, size, and ultrasound patterns. This analytical strength differentiates our work from numerous prior studies that primarily reported univariate associations. For example, while previous studies noted the presence of features like tentacle-like projections or hypervascularity, our model quantified their independent predictive power while simultaneously by integrating other variables like tumor size and location. These findings align with established clinical risk factors and should prompt suspicion for DF or DFSP when present. Typical DF cases with characteristic clinical and sonographic features, such as girdle, limb, and small size, may be managed conservatively, while lesions showing DFSP characteristic clinical and sonographic features, such as large size, tentacle-like border pattern, internal hyperechoic area, peripheral hyperechoic rim, and mixed echogenicity pattern, warrant biopsy and wide excision with 2–3 cm margins due to their aggressive potential.[26] For different anatomical sites, selecting the appropriate pedicled or free flap for reconstruction after wide excision ensures good functional and aesthetic outcomes with no local recurrence.[27–30]

Both HFUS and UHFUS aid preoperative planning, which achieve 81.8% sensitivity for detecting muscle invasion, potentially reducing incomplete excisions and recurrence.[31] From a clinical management perspective, the multivariate model provides a practical tool for risk stratification. The strong association of girdle and limb location with DF suggests

that ultrasound identification of a small lesion on the girdle or limb may allow for watchful waiting in clinically typical cases. In contrast, the identification of a large, lesion on the trunk with a tentacle-like border pattern, internal hyperechoic area, peripheral hyperechoic rim or mixed echogenicity pattern should be considered highly suspicious for DFSP, mandating definitive histological diagnosis and surgical consultation. This predictive model can help clinicians prioritize higher-risk lesions for expedited intervention, potentially improving outcomes by reducing time to treatment for aggressive tumors.

Our systematic classification of DF and DFSP using HFUS and UHFUS revealed strong correlations with histopathology and clinical behavior. The localized pattern (65.2% of DF cases) appears as a well-defined hypoechoic nodule, consistent with circumscribed growth. The serrated pattern (18.4% of DF cases) shows heterogeneous echogenicity with serrated structures, requiring differentiation from early DFSP.[32] The tentacle-like border pattern, more frequent in DFSP (17.3% of DFSP cases), is caused by tumor cells spreading along the fat septum, indicating infiltrative growth and necessitating wide excision.[33,34] Peripheral hyperechoic rim (11.8% of DFSP cases) likely indicates involvement of surrounding adipose tissue by the lesion, while the internal hyperechoic pattern (23.6% of DFSP cases) represents the invasion and encasement of adipose tissue by the lesion, both of which likely reflect collagen deposition or necrosis, enhancing diagnostic specificity.[10,35] The mixed echogenicity pattern (18.9% of DFSP cases) underscores tumor heterogeneity, likely stemming from the intricate interweaving of tumor cell bundles and collagen fibers.

Limitations and Future Directions

This study has several limitations that should be considered when interpreting the results. As a single-center retrospective analysis spanning 15 years, the extended timeframe may have introduced variability in image acquisition and interpretation. It is also important to note that a small subset of patients did not undergo ultra-high frequency ultrasound examination. Although the initial cohort was large, the final analytical sample was substantially reduced, partly due to limited clinician familiarity with cutaneous ultrasound which led to the underutilization of such examinations prior to lesion excision, raising the possibility of selection bias. Furthermore, it is important to note that the initial univariate screening involved a substantial number of comparisons without formal statistical correction, which may increase the risk of Type I error (false positives). These univariate results were used solely for the purpose of informing variable selection for the subsequent multivariate model and should be interpreted with this caveat in mind.

Future research should aim to address these limitations. Prospective, multi center studies using standardized ultrasound protocols and equipment are needed to validate our findings and enhance their generalizability. Efforts to increase clinician awareness and training in cutaneous ultrasound could help mitigate selection bias in future patient recruitment. Furthermore, the integration of advanced multimodal ultrasound techniques, such as elastography and contrast enhanced ultrasound, which the existing literature suggests hold significant potential for improving diagnostic accuracy, should be prioritized.[34,36,37] Finally, incorporating artificial intelligence and explainable artificial intelligence models could help overcome challenges related to variable interpretation and multicollinearity by standardizing image analysis and identifying the most salient diagnostic features.[38] By combining refined ultrasound examinations with these emerging technologies, future work can advance the development of robust, personalized diagnostic strategies to improve patient outcomes.

Conclusion

This 15-year retrospective analysis demonstrates that ultrasound, particularly at higher frequencies, is a powerful, non-invasive tool for characterizing dermatofibrosarcoma protuberans (DFSP) and dermatofibroma (DF). DFSP lesions are typically larger, located on the trunk, and exhibit distinct sonographic features, including heterogeneity, tentacle-like borders, peripheral hyperechoic rims, mixed echogenicity, and marked hypervascularity. In contrast, DF is more common on the extremities, is smaller, and often appears homogeneous with compressive or serrated patterns. Multivariate analysis confirmed that tumor location, larger size, and specific ultrasound patterns are independent predictors. These sonographic findings provide critical preoperative diagnostic information, guiding appropriate clinical management with conservative approaches for DF and wide surgical excision for DFSP. Future multi-center studies are warranted to

validate these criteria, and the integration of artificial intelligence could further enhance diagnostic standardization and accuracy.

Transparency Statement

We can confirm that this manuscript is an honest, accurate, and transparent account of the case being reported and that no important aspects of the case have been omitted.

Abbreviations

DF, Dermatofibroma; DFSP, Dermatofibrosarcoma protuberans; HFUS, High-frequency ultrasound; UHFUS, Ultra-high-frequency ultrasound; OR, Odds ratio; CI, Confidence interval; VIF, variance inflation factor.

Data Sharing Statement

The data used to support the findings of this study are available from the corresponding author upon request.

Ethical Approval and Consent to Participate

This retrospective study was conducted in accordance with the Declaration of Helsinki and was approved by the Dongguan People's Hospital Ethics Committee (KYKT2021-048). The requirement for individual patient informed consent was waived by the ethics committee as the study involved only retrospective analysis of archived medical records. All patient data were handled with strict confidentiality, and personal identifiers were removed to protect patient privacy throughout the research process.

Author Contributions

All authors made a significant contribution to the work reported, whether that is in the conception, study design, execution, acquisition of data, analysis and interpretation, or in all these areas; took part in drafting, revising or critically reviewing the article; gave final approval of the version to be published; have agreed on the journal to which the article has been submitted; and agree to be accountable for all aspects of the work.

Funding

No funding was received for this study.

Disclosure

The authors declare that they have no conflicts of interest.

References

1. Kawaguchi M, Kato H, Noda Y, et al. Imaging findings of malignant skin tumors: radiological-pathological correlation. *Insights Imaging*. 2022;13(1):52. doi:10.1186/s13244-022-01205-8
2. Hao X, Freedman D, Yim J, et al. Dermatofibromas on the foot and ankle: a clinicopathologic characterization of 31 cases. *J Am Podiatr Med Assoc*. 2024;114(3):21–207. doi:10.7547/21-207
3. Peng Q, Lu Y, Su T, et al. Dermatofibrosarcoma protuberans: a clinical and pathological observational report of Asian samples from one center. *J Cancer Res Ther*. 2024;20(7):2035–2040. doi:10.4103/jcrt.jcrt_2661_23
4. Khamdan F, Brailsford C, Dirr MA, et al. Dermatofibroma versus dermatofibrosarcoma protuberans: a nuclear morphology study. *Am J Dermatopathol*. 2023;45(9):631–634. doi:10.1097/DAD.0000000000002526
5. Saiag P, Lebbe C, Brochez L, et al. Diagnosis and treatment of dermatofibrosarcoma protuberans. European interdisciplinary guideline - update 2024. *Eur J Cancer*. 2025;218:115265. doi:10.1016/j.ejca.2025.115265
6. Russo A, Reginelli A, Lacasella GV, et al. Clinical application of ultra-high-frequency ultrasound. *J Pers Med*. 2022;12(10):1733. doi:10.3390/jpm12101733
7. Granieri G, Oranges T, Morganti R, et al. Ultra-high frequency ultrasound detection of the dermo-epidermal junction: its potential role in dermatology. *Exp Dermatol*. 2022;31(12):1863–1871. doi:10.1111/exd.14664
8. Zhang YQ, Wang LF, Ni N, et al. The value of ultra-high-frequency ultrasound for the differentiation between superficial basal cell carcinoma and Bowen's disease. *Dermatology*. 2023;239(4):572–583. doi:10.1159/000529448
9. Choi JY, Park HJ, Kim JN, et al. Can ultrasound distinguish between dermatofibroma and subcutaneous epidermal tumors? - Imaging features and reproducibility. *Clin Imaging*. 2021;79:52–55. doi:10.1016/j.clinimag.2021.03.036

10. Won KY, Park SY, Jin W, et al. Dermatofibroma: sonographic findings and pathologic correlation. *Acta Radiol*. 2018;59(4):454–459. doi:10.1177/0284185117721263
11. Whittle C, Andrews A, Coulon G, et al. Different sonographic presentations of dermatofibrosarcoma protuberans. *J Ultrasound*. 2024;27(1):61–65. doi:10.1007/s40477-023-00796-2
12. Gong X, Li J, Ding A, et al. Multimodal ultrasound for preoperative evaluation of dermatofibrosarcoma protuberans: a series of 40 cases. *BMC Cancer*. 2022;22(1):1137. doi:10.1186/s12885-022-10211-4
13. Brailsford C, Khamdan F, Dirr MA, et al. A study of collagen refractility in dermatofibroma and dermatofibrosarcoma protuberans using diffractive microscopy. *J Cutan Pathol*. 2024;51(4):306–310. doi:10.1111/cup.14577
14. Miao Y, Ren WW, Yang FY, et al. Diagnostic value of high-frequency ultrasound (HFUS) in evaluation of subcutaneous lesions. *Skin Res Technol*. 2023;29(9):e13464. doi:10.1111/srt.13464
15. Aytekin S, Kaynak E, Ayhan E. Dermoscopy of dermatofibromas: a new perspective. *Int J Clin Pract*. 2021;75(10):e14547. doi:10.1111/ijcp.14547
16. Pogorzelska-Antkowiak A, Wcisło-Dziadecka D, Brzezińska-Wcisło L, et al. Features of dermatofibroma in reflectance confocal microscopy. *Int J Dermatol*. 2020;59(8):951–954. doi:10.1111/ijd.14972
17. Apalla Z, Liopyris K, Kyrmanidou E, et al. Clinical and dermoscopic characteristics of cutaneous sarcomas: a literature review. *Diagnostics*. 2023;13(10):1822. doi:10.3390/diagnostics13101822
18. Mustari A, Chauhan P, Chatterjee D, et al. Dermoscopy of dermatofibrosarcoma protuberans in skin of colour: a study of four cases. *Indian J Dermatol Venereol Leprol*. 2024;90(6):801–803. doi:10.25259/IJDVL_325_2023
19. Choi ME, Lee M, Lee WJ, et al. Clinical and histopathological analysis of 141 dermatofibrosarcoma protuberans in Korea: a comparative study according to trauma. *Australas J Dermatol*. 2022;63(4):e297–e304. doi:10.1111/ajd.13920
20. Zhang Y, Zhu L, Guo Y, et al. Clinical and histopathological characteristics of atrophic pigmented dermatofibrosarcoma protuberans: a retrospective study of 14 cases. *Heliyon*. 2024;10(22):e39271. doi:10.1016/j.heliyon.2024.e39271
21. Li D, Yang F, Zhao Y, et al. High-frequency ultrasound imaging to distinguish high-risk and low-risk dermatofibromas. *Diagnostics*. 2023;13(21):3305. doi:10.3390/diagnostics13213305
22. Binișor I, Baniță IM, Alexandru D, et al. Progranulin: a proangiogenic factor in visceral adipose tissue in tumoral and non-tumoral visceral pathology. *Exp Ther Med*. 2021;22(5):1337. doi:10.3892/etm.2021.10772
23. Ren Q, Li J, Shangguan J, et al. Imaging features of dermatofibrosarcoma protuberans. *J Cancer Res Ther*. 2022;18(2):476–481. doi:10.4103/jcrt.jcrt_1619_21
24. Gimeno-Ribes ME, Toll A, Garcia A, et al. Usefulness of high-frequency Doppler ultrasound in dermatofibrosarcoma protuberans. *J Ultrasound Med*. 2023;42(9):2171–2173. doi:10.1002/jum.16217
25. Zou MH, Huang Q, Yang T, et al. Role of ultrasound in the diagnosis of primary and recurrent dermatofibrosarcoma protuberans. *BMC Cancer*. 2021;21(1):909. doi:10.1186/s12885-021-08476-2
26. Sanchez-Diaz M, Martinez-Lopez A, Montero-Vilchez T, et al. Ultrasonography as a novel technique for intraoperative delimitation of dermatofibrosarcoma protuberans. *Dermatol Surg*. 2022;48(5):575–577. doi:10.1097/DSS.0000000000003404
27. Longo B, Paolini G, Belli E, et al. Wide excision and anterolateral thigh perforator flap reconstruction for dermatofibrosarcoma protuberans of the face. *J Craniofac Surg*. 2013;24(6):e597–e599. doi:10.1097/SCS.0b013e3182a238c1
28. Longo B, D'orsi G, Orlando G, et al. Recurrent dermatofibrosarcoma protuberans of the clavicular region: radical excision and reconstruction with latissimus dorsi myocutaneous flap. *PRRS*. 2022;1:14–19. doi:10.57604/PRRS-002
29. Hsieh PJ, Shi MY, Pu CM. Subtotal thigh flap for large abdominal wall defect reconstruction in patient with recurrent dermatofibrosarcoma protuberans: a case report and literature review. *Ann Plast Surg*. 2024;92(1S Suppl 1):S41–S44. doi:10.1097/SAP.0000000000003785
30. Lim MC, Halim AS. Dermatofibrosarcoma protuberans post excision reconstruction options and outcome: 10 years single center experience. *J Plast Reconstr Aesthet Surg*. 2025;104:139–145. doi:10.1016/j.bjps.2025.02.034
31. Liu Y, Huang K, Chen M, et al. High-frequency ultrasound-assisted Mohs micrographic surgery for the treatment of dermatofibrosarcoma protuberans. *J Plast Reconstr Aesthet Surg*. 2024;96:186–195. doi:10.1016/j.bjps.2024.07.013
32. Dong B, Xia H, Liu Y, et al. Evaluation of very-high-frequency ultrasound imaging characteristics of dermatofibroma. *Clin Cosmet Invest Dermatol*. 2024;17:2795–2802. doi:10.2147/CCID.S493437
33. Diago A, Llombart B, Serra-Guillen C, et al. Usefulness of ultrasound in dermatofibrosarcoma protuberans and correlation with histopathological findings: a series of 30 cases. *Skin Res Technol*. 2021;27(5):701–708. doi:10.1111/srt.13003
34. Zhang Y, Liang JF, Luo PP, et al. High-frequency ultrasound and shear wave elastography of dermatofibrosarcoma protuberans: a novel approach for early detection. *J Clin Ultrasound*. 2025;53(5):1035–1044. doi:10.1002/jcu.23978
35. Schechter SA, Bresler SC, Patel RM. Fat necrosis with an associated lymphocytic infiltrate represents a histopathologic clue that distinguishes cellular dermatofibroma from dermatofibrosarcoma protuberans. *J Cutan Pathol*. 2020;47(10):913–916. doi:10.1111/cup.13744
36. Gong X, Li J, Ding A, et al. Conventional and contrast-enhanced ultrasound in the differential diagnosis of recurrent dermatofibrosarcoma protuberans and postoperative scar. *BMC Cancer*. 2024;24(1):285. doi:10.1186/s12885-024-11991-7
37. Bezpalko L, Filipskiy A. Clinical and ultrasound evaluation of skin quality after subdermal injection of two non-crosslinked hyaluronic acid-based fillers. *Clin Cosmet Invest Dermatol*. 2023;16:2175–2183. doi:10.2147/CCID.S402409
38. Hauser K, Kurz A, Haggenmüller S, et al. Explainable artificial intelligence in skin cancer recognition: a systematic review. *Eur J Cancer*. 2022;167:54–69. doi:10.1016/j.ejca.2022.02.025